Published in final edited form as:
Plant J. 2012 February ; 69(4): 655–666. doi:10.1111/j.1365-313X.2011.04820.x.

The fruit cuticles of wild tomato species exhibit architectural and chemical diversity, providing a new model for studying the evolution of cuticle function

Trevor H. Yeats[1], **Gregory J. Buda**[1], **Zhonghua Wang**[2], **Noam Chehanovsky**[3], **Leonie C. Moyle**[4], **Reinhard Jetter**[2,5], **Arthur A. Schaffer**[3], and **Jocelyn K.C. Rose**[1,*]

[1]Department of Plant Biology, Cornell University, Ithaca, NY 14853, U.S.A.

[2]Department of Botany, University of British Columbia, Vancouver, BC V6T 1Z4, Canada

[3]Institute of Field and Garden Crops, ARO, The Volcani Center, Bet Dagan 50250, Israel

[4]Department of Biology, Indiana University, Bloomington, IN, 47405 U.S.A.

[5]Department of Chemistry, University of British Columbia, Vancouver, BC V6T 1Z4, Canada

Summary

The cuticle covers the aerial epidermis of land plants and plays a primary role in water regulation and protection from external stresses. Remarkable species diversity in the structure and composition of its components, cutin and wax, have been catalogued, but few functional or genetic correlations have emerged. Tomato (*Solanum lycopersicum*) is part of a complex of closely related wild species endemic to the northern Andes and the Galapagos Islands (*Solanum* Sect. *Lycopersicon*). Although sharing an ancestor less than seven million years ago, these species are found in diverse environments and are subject to unique selective pressures. Furthermore, they are genetically tractable, since they can be crossed with *S. lycopersicum*, which has a sequenced genome. With the aim of evaluating the relationships between evolution, structure and function of the cuticle, we characterized the morphological and chemical diversity of fruit cuticles of seven species from *Solanum* Sect. *Lycopersicon*. Striking differences in cuticular architecture and quantities of cutin and waxes were observed, with wild species wax coverage exceeding that of *S. lycopersicum* by up to seven fold. Wax composition varied in the occurrence of wax esters and triterpenoid isomers. Using a *S. habrochaites* introgression line population, we mapped triterpenoid differences to a genomic region that includes two *S. lycopersicum* triterpene synthases. Based on known metabolic pathways for acyl wax compounds, hypotheses are discussed to explain the appearance of wax esters with atypical chain lengths. These results establish a model system for understanding the ecological and evolutionary functional genomics of plant cuticles.

Keywords

fruit; cuticle; cutin; wax; introgression lines; metabolic profiling; *Solanum lycopersicum*; tomato wild species

*Corresponding author: (fax +1 607 255 5407; tel +1 607-255 4781; jr286@cornell.edu).

Introduction

The plant cuticle is a waxy surface layer covering the primary aerial organs of all land plants. While it is central to limiting non-stomatal water loss, it is now clear that the cuticle plays a myriad of roles as the primary interface between the plant and its environment. It is an effective barrier against pests and pathogens (Reina-Pinto and Yephremov, 2009), shields the plant from excessive UV radiation (Pfündel *et al.*, 2006) and can act as a self-cleaning surface (Barthlott and Neinhuis, 1997). It also has a critical function in plant development, by establishing boundaries between nascent organs (Javelle *et al.*, 2011).

The hydrophobic cuticle is contiguous with the polysaccharide cell wall and consists primarily of a lipid polymer, cutin, and a variety of organic solvent-soluble compounds that are collectively termed waxes. Cutin is a polyester of ω- and midchain-substituted fatty acids and three main types exist, based on the predominant chain length of fatty acids and the nature of the substitutions. C16-type cutins are typically rich in dihydroxyhexadecanoic acid with midchain- and 16-hydroxy groups, while C18-type cutins are principally composed of 9,10-epoxy-18-hydroxyoctadecanoic acid or 9,10,18-trihydroxyoctadecanoic acid (Kolattukudy, 2001). More recently, analysis of arabidopsis (*Arabidopsis thaliana*) stem and leaf cutin identified a third type of cutin that is rich in C18 dicarboxylic acids (Bonaventure *et al.*, 2004; Franke *et al.*, 2005). Finally, although not typically detected for technical reasons, glycerol is found in varying abundance in the cutin polymers of many species (Graca *et al.*, 2002).

Waxes accumulate within the cutin matrix as intracuticular waxes, and they are also deposited on the outer surface of the cuticle as epicuticular crystals or films (Buschhaus and Jetter, 2011). Wax mixtures are typically more complex and variable than cutin, but broadly consist of homologous series of acyl lipids, derived from very-long-chain fatty acids (VLCFAs), and a variety of other lipophilic metabolites. The acyl lipids include alkanes, fatty acids, alcohols and wax esters, the occurrence and abundance of which vary between species and during ontogeny (Jenks and Ashworth, 1999). Examples of non-acyl wax compounds are pentacyclic triterpenoids, flavonoids and tocopherols, although their incidence is even more variable (Jetter *et al.*, 2006).

Fossil evidence suggests that evolution of a cuticle was one of the primary adaptations that allowed plants to colonize land, with both morphological and chemical evidence of the first cuticles dating to the late Silurian and early Devonian periods (Edwards, 1993; Niklas, 1980). Over the last four hundred million years substantial diversification in cuticle morphology and composition has occurred (Jeffree, 2006; Walton, 1990); however, attempts to correlate this variation with functional characteristics of the cuticle have had mixed success. On one hand, the self-cleaning of the plant surface by water beading, known as the lotus effect, was correlated with deposition of epicuticular wax crystals through a survey of ~ 10,000 diverse species (Barthlott and Neinhuis, 1997). On the other hand, the intuitive correlations between cuticle thickness or wax amount, and cuticular water permeability were not confirmed by a survey of the cuticles of 23 species (Riederer and Schreiber, 2001). However, it is important to note that such taxonomic comparisons have largely involved distantly related species, in the absence of genetic resources, thus limiting molecular interpretation of cuticular diversity, while molecular models for cuticle biosynthetic pathways have mostly resulted from studies of mutants in model systems such as arabidopsis (Kunst and Samuels, 2009; Pollard *et al.*, 2008).

In order to resolve the complex interaction between cuticle structures, functions and evolution, a promising approach lies in the emerging discipline of ecological and evolutionary functional genomics (EEFG; Mitchell-Olds *et al.*, 2008). A prerequisite for this

approach is a set of species with diverse ecological preferences, but with relatively recent evolutionary divergence, as well as access to the genomic tools of a model organism. For EEFG studies of the plant cuticle, an excellent model is presented by the wild relatives of tomato (*S. lycopersicum*). This group of approximately 14 species, *Solanum* Sect. *Lycopersicon*, evolved from a common ancestor less than seven million years ago and today is endemic to an array of environments in the northern Andes and Galapagos Islands (Peralta *et al.*, 2008). Furthermore, they can be crossed with *S. lycopersicum* and share a high degree of genomic synteny, allowing the sequenced genome of *S. lycopersicum* and its associated genomic resources to be utilized (Mueller *et al.*, 2005). A particularly useful resource for comparative genetic studies is the availability of several introgression line (IL) populations, consisting of discrete marker-defined homozygous segments of wild species chromosomes in a *S. lycopersicum* background (Prudent *et al.*, 2009; Monforte and Tanksley, 2000; Eshed and Zamir, 1995).

In addition to the advantages of *Solanum* Sect. *Lycopersicon* as an EEFG model system, tomato is an excellent experimental resource for cuticle biology in its own right. The tomato fruit cuticle is particularly substantial, enabling detailed morphological analysis by light microscopy (Buda *et al.*, 2009), as well as easy isolation of a completely intact membrane, facilitating both biomechanical and chemical analysis. Additionally, the fruit epidermis is astomatous, greatly simplifying any tests of cuticular permeability. Finally, both the wax and cutin of tomato fruits have relatively simple compositions (Baker *et al.*, 1982).

To test the hypothesis that *Solanum* Sect. *Lycopersicon* represents a valuable EEFG model system for cuticle biology, we characterized the cuticular morphology and composition of seven of these species, which were selected to span the range of evolutionary history, geography and environment in *Solanum* Sect. *Lycopersicon* (Figure 1). Previous surveys of the chemical composition of fruits of *Solanum* Sect. *Lycopersicon* have uncovered diversity in a wide range of metabolites (Schauer, *et al.* 2005) but neither the chemistry nor the morphology of fruit cuticles has yet been studied. While the cuticle may, at least in some plant species, be subject to dynamic adaptation to environmental stresses (Kosma *et al.*, 2009), for this study we first focused on establishing the static features of the cuticle by growing all tomato species in the same greenhouse conditions. We present the remarkable architectural and chemical diversity exhibited by cuticles of the wild relatives of tomato, and demonstrate the value of existing genetic resources to identify the molecular basis of the underlying compositional diversity.

Results

Two-dimensional Cuticle Morphology

In order to characterize the structural features of the fruit cuticles, isolated fruit pericarp cryosections were prepared and observed with differential interference contrast (DIC) light microscopy (Figure 2a–g). In *S. lycopersicum, S. pimpinellifolium* and *S. cheesmaniae* (Fig 2a–c, respectively), a flat surface topology was observed, with well developed anticlinal pegs (APs) between the epidermal cells. The APs of *S. pimpinellifolium* are particularly pronounced: the epidermal cells adopt a nearly conical shape and the anticlinal cell wall is nearly filled by substantial but tapered pegs (Figure 2b). In the remaining species, a papillate surface topology was observed, generally leading to the incorporation of the AP structures into the continuous undulating organization of the cuticle (Figure 2d–g). *S. habrochaites* has an intermediate architecture, where the papillate morphology is less pronounced and APs are present, but only to half the depth of the epidermal cells (Figure 2f). The occurrence of subepidermal cuticular deposits (SD) correlates with the appearance of APs (Fig 2a–g), with *S. pimpinellifolium* exhibiting the greatest degree of cuticle accumulation in both of these locations (Figure 2b).

To complement the qualitative observations of cuticle structure, the cuticle thickness above each epidermal cell was quantified (Figure 2h). The two sister species *S. habrochaites* and *S. pennellii* had the thinnest cuticles, each with an average thickness of ~4 μm, while another set of sister species, *S. neorickii* and *S. chmielewskii*, had the thickest cuticles, with an average thickness of ~7 μm.

Three-dimensional Cuticle Morphology

Since preliminary analysis by DIC microscopy showed considerable diversity in cuticle structure, cuticle morphology was further investigated for several of the species using three-dimensional confocal microscopy. Thick sections (30 μm) of fruit pericarp material were prepared by cryosectioning and stained with Auramine O. A series of optical sections were collected using a confocal scanning laser microscope and these were assembled into three-dimensional volume renderings. Using this technique, we were able to clearly observe a number of unique topological features that were either subtle or invisible by DIC microscopy.

In *S. pimpinellifolium* sections, the APs were divided down the middle by more lightly stained and presumably more polar anticlinal lamellae (AL) (Figure 3b,c). These clearly outlined the anticlinal boundary of each cell (Figure 3c). In species with papillate surface topology, this could be seen in striking relief (Figure 3d–k). Moreover, the internal surface topology (IST) was revealed. *S. habrochaites* has a particularly rough IST consisting of fused spherical globules of ~1 μm diameter (Figure 3g, h). In contrast, the IST of *S. neorickii* and *S. pennellii* were relatively smooth (Figure 3e, k).

Scanning electron microscopy (SEM) was used on a subset of species in order to confirm the structural features that were observed by light and confocal microscopy. While the papillate surface topology of *S. chmielewskii* and *S. habrochaites* was readily visible using SEM, the internal surface topology could not be observed, nor was it possible to distinguish between the cuticular membrane and the polysaccharide cell wall (Figure S1).

Cutin chemical analysis

The predominant component of the tomato fruit cuticle is cutin, which typically exceeds the mass of wax by nearly 100-fold (Baker *et al.*, 1982). Thus, the major lipids stained in our microscopic analysis corresponded to the cutin polymer. To characterize the cutin in more detail, the fruit cuticular membranes from each species were enzymatically isolated, extracted of wax and depolymerized by methanolysis. The resulting methyl esters of cutin monomers were identified by GC-MS and quantified by GC-FID (Figure 4).

In terms of overall quantity of cutin identified, the chemical analysis generally confirmed the pattern based on microscopic thickness measurements (Figure 2h). However, a major exception is *S. pimpinellifolium*, which exhibits nearly twice the cutin load, while having nearly the same thickness as *S. lycopersicum*. This discrepancy is likely accounted for by the cutin in the thick APs of this species (Figure 2b, Figure 3b, c). Another notable result of comparing the microscopy images with the chemical analysis is the fact that, while *S. pennellii* and *S. habrochaites* both have similar cuticular thickness and architecture (Figure 2f–h), the cuticle of *S. habrochaites* is nearly three times as rich in cutin as *S. pennellii*.

In terms of cutin monomer composition, the most notable trend was the enhanced levels of 9,10,18-trihydroxyoctadecanoic acid in three species. While this monomer accounted for 6%, 10% and 6% of the cutin in *S. chmielewskii, S. habrochaites* and *S. pennellii*, respectively, it corresponded to less than 3% of the cutin in the remaining species (Figure 4).

Wax chemical analysis

Wax extracts from the isolated cuticles were analyzed by gas chromatography coupled to mass spectrometry and flame ionization detector (GC-MS and CG-FID). All wild species accumulated more wax than *S. lycopersicum*, although only three species (*S. chmielewskii, S. neorickii* and *S. pennellii*) show substantially greater wax levels (Figure 5a). The wax coverage of *S. neorickii* is particularly remarkable and exceeds that of *S. lycopersicum* by nearly seven-fold.

Considering the wax composition, alkanes represented the majority of identified compounds in all species (Figure 5a). Within the homologous series of *n*-alkanes, the typical predominance of odd chain lengths was observed in all species (Figure 5b), with the most common chain length being C31, except in *S. chmielewskii, S. neorickii* and *S. habrochaites*, where C29 was the most abundant (Figure 5b). In the same three species, alkyl esters were detected, accounting for 7–20% of the wax (Figure 5a). Alkyl esters typically show a chain length distribution favoring even chain lengths (Jetter *et al.*, 2006), but for the three species where alkyl esters were observed, relatively little even bias was seen (Figure 5c). To further investigate whether the unexpected abundance of odd-chain lengths was due to contributions from the fatty acid or alcohol moiety, wax extracts from *S. neorickii* were fractionated by thin layer chromatography (TLC) and the ester fraction was recovered and methanolyzed. GC analysis showed the esters to be composed of C16-C28 fatty acids that were mostly even in chain length, and C22-C30 alcohols of both even and odd chain lengths (Figure S2).

Across the species, the major non-aliphatic compounds observed were the pentacyclic triterpenoids, accounting for 1–35% of the total wax, although they could not be detected in *S. pennellii* (Figure 5a). The predominant isomers observed were α-amyrin, β-amyrin and δ-amyrin, with Ψ-taraxasterol and taraxasterol appearing at much lower levels. In *S. habrochaites*, β-amyrin was the only pentacyclic triterpenoid that was detected (Figure 5d).

Genetic mapping of cuticle traits using IL populations

As a demonstration of using ILs to genetically map cuticular traits, we focused on understanding the genetic basis for the absence of non-β-amyrin triterpenoid isomers in *S. habrochaites*. We isolated cuticular wax from a collection of 51 *S. habrochaites* ILs that collectively cover nearly the entire *S. habrochaites* genome (Monforte and Tanksley, 2000). GC analysis revealed that the wax extracts of these lines all had a similar triterpenoid isomer composition to the *S. lycopersicum* parent with the exception of line LA3917, the triterpenoid profile of which consisted almost entirely of β-amyrin (Figure 6a). This line contains two unique DNA segments on chromosomes 1 and 12 that are not present in any of the other lines examined. The segment on the end of chromosome 12 includes the tandem loci *SlTTS1* and *SlTTS2* that encode the two triterpenoid synthases responsible for biosynthesis of the entire array of triterpenoid isomers that are observed in *S. lycopersicum* (Figure 6b). SlTTS1 specifically synthesizes β-amyrin, while SlTTS2 is a multifunctional synthase with δ-amyrin as its most abundant product (Figure 6c; Wang *et al.*, 2011).

Discussion

Cuticle Morphology

The microscopic morphology of the fruit cuticle and the underlying epidermal cell layer was strikingly variable between the seven tomato species examined, despite relatively little variation in overall cuticle thickness (Figure 2). We observed no association between climatic factors (e.g. mean annual temperature and precipitation) and cuticular thickness (Figures 1 and 2), which is consistent with previous results showing no correlation between

cuticle thickness and water permeability in a survey of taxonomically diverse species (Riederer and Schreiber, 2001) and a study of tomato mutants with varying degrees of fruit cutin deficiency (Isaacson *et al.*, 2009).

There is a general trend of a flat rather than undulating cuticle surface in species most closely related to *S. lycopersicum* (Figures 2 and 3), which would have a substantial effect on surface area and cuticular water conductance. For example, measurement of the surface following the two dimensional contour of the epidermis of *S. chmielewskii*, rather than the straight line assumed by approximating the surface area of a sphere, indicates that the effective surface area is ~50% greater. The effective cuticular transpiration, expressed as the flux of water across the epidermal surface, would thus be significantly affected by the cuticular topology on the cellular scale.

Previous studies of quantitative trait loci (QTL) derived from *S. chmielewskii* identified several QTL associated with increased or decreased fruit cuticular water permeability (Prudent *et al.*, 2009). The differences associated with these QTL were on the same order of magnitude as the ~50% difference in microscopic surface area and the ~200% difference in wax load that we observed in comparing *S. lycopersicum* and *S. chmielewskii* (Figures 2 and 5). It is likely that the variation in cuticular water permeability that was observed, considering macroscopic surface area, was due to either variation in cuticular morphology, or wax amount and composition. Along these lines, the previously described *Cwp1* genotype, containing a *S. habrochaites* allele of this gene that is expressed in the *S. lycopersicum* background, had enhanced cuticular water permeability that was associated not with altered cuticle chemistry, but rather with microfissures within the cuticle (Hovav *et al.*, 2007).

If variation in cuticular morphology were shaped by adaptive responses to environmental variation, one expectation might be that a lower surface area would be favored in species endemic to warm and dry environments. Indeed, this trend is observed with all the species except *S. pennellii*, which is endemic to regions with the lowest precipitation conditions of all the species considered, and yet features an undulating cuticle (Figures 1 and 2). Interestingly, *S. pennellii* frequently occurs in ‘lomas formations’; mid-elevation fog-zone locations that have low precipitation but high ambient humidity (Dillon, 1989). Such a unique climatic condition might explain this anomalous observation. Clearly, many factors are important for determining cuticular water permeability. Wax composition and amount are often discussed as principal determinants of cuticular water permeability (Jenks and Ashworth, 1999) and pubescent surfaces, such as that of *S. habrochaites*, can also contribute to the transpirational barrier (Fernández *et al.*, 2011). However, from both a technical and evolutionary perspective, the microscopic topology of the cuticle surface appears to be an important factor.

Cutin

The total amount of fruit cutin coverage varied from a low of 175 μg cm^{-2} in *S. pennellii* to a maximum of 950 μg cm^{-2} in *S. pimpinellifolium*. There was no association between climate factors and cutin amount, further suggesting the model that wax, and not cutin, is the major determinant of cuticular water permeability in tomato fruit (Isaacson *et al.*, 2009; Leide *et al.*, 2007). In terms of composition, there were few differences between the species, with the exception of the abundance of 9,10,18-trihydroxy octadecanoic acid, which accounts for 6–10% of the cutin in *S. habrochaites, S. pennellii* and *S. chmielewskii* but less than 3% of cutin in the other species. This monomer is widely distributed in plant cutins, and is one of the representative monomers of C18-type cutins (Kolattukudy, 2001). Radioactive feeding experiments with *cis-9*-octadecenoic acid have indicated that biosynthesis of 9,10,18-trihydroxy octadecanoic acid in *Spinacia oleracea* likely occurs by

ω-hydroxylation of *cis-9*-octadecenoic acid followed by introduction of an epoxy group at the double bond by a cytochrome P450 epoxidase (Croteau and Kolattukudy, 1975a; Kolattukudy *et al.*, 1973). The resulting compound, 9,10-epoxy-18-hydroxyoctadecanoic acid is itself a common monomer of some cutin and suberin polymers, and for *Malus pumila* it was shown that opening of the epoxide ring to yield 9,10,18-trihydroxy octadecanoic acid likely occurs through the action of epoxide hydrolase enzymes (Croteau and Kolattukudy, 1975b). It can be assumed that the same enzymatic reactions lead to formation of the trihydroxy fatty acid monomer found in tomato fruit cutin (Figure 7).

The genes encoding several of the cytochrome P450s involved in cutin biosynthesis have been identified by studying arabidopsi*s* mutants. The fatty acid ω-hydroxylase activity is encoded by genes of the CYP86 family (Pinot and Beisson, 2011), while a mid-chain hydroxylase is encoded by CYP77A6 (Li-Beisson *et al.*, 2009). Biochemical characterization of another member of the CYP77 family, CYP77A4, showed that, in addition to possessing a mid-chain hydroxylase activity, the enzyme also has epoxidase activity on unsaturated substrates (Sauveplane *et al.*, 2009).

Taken together, the current model for the synthesis of C18 mid-chain epoxy and trihydroxy cutin monomers involves CYP86 catalyzing ω-hydroxylation of an unsaturated substrate followed by epoxidation catalyzed by CYP77. In the species that we examined here, the increased prevalence of this pathway (as opposed to C16 monomer biosynthesis) could potentially occur through an increased C18 desaturase activity, or altered substrate specificity of the CYP86 ω-hydroxylase (Figure 7). Future work identifying the genetic basis of this shift to C18 monomers could be interesting as they have a greater potential for forming dendritic structures that may alter the cutin polymeric structure (Pollard *et al.*, 2008).

Wax

The most striking observation regarding the cuticular wax of the species examined was the extremely high abundance of wax in *S. neorickii*, which was seven-fold higher than in *S. lycopersicum* (Figure 5a). It is tempting to draw the intuitive correlation between this dramatically increased wax accumulation and adaptation to an arid environment. However, *S. neorickii* is endemic to cooler and moister environments than the other species studied, with the exception of the closely related *S. chmielewskii* (Figure 1c). On the other hand, desiccating conditions may occur on smaller geographical scales and can depend on factors such as soil drainage, wind and altitude that are not accounted for when only considering average precipitation and temperature. Future studies looking at co-occurrence of wax accumulation and cuticular water permeability QTL could provide new insight into the functional significance of increased wax accumulation. There is emerging evidence of genetic programs for enhanced wax production during drought stress (Seo *et al.*, 2011; Kosma *et al.*, 2009) and constitutive activation of these pathways could be an adaptive strategy for tolerating persistent water stress.

We observed a correlation between decreasing prevalence of triterpenoids and phylogenetic distance from *S. lycopersicum*, with *S. pennellii* exhibiting no detectable triterpenoids (Figure 5.) Previous studies of tomato mutants have indicated that triterpenoids do not contribute to the water barrier properties of a cuticle (Vogg *et al.*, 2004; Leide *et al.*, 2007), suggesting that aliphatic, rather than triterpenoid, compounds would be favored in species adapted to arid environments. With the exception of *S. pimpinellifolium*, which is endemic to one of the warmer and drier environments, our results might suggest a role for aliphatic compounds in dry adaptation for some species (Figures 1 and 5), but this has yet to be tested experimentally.

Identification of an unusual wax ester profile

The final wax-related trend was the appearance of wax esters in three of the species, *S. chmielewskii, S. neorickii* and *S. habrochaites*. These are typical components of cuticular wax from many species, but they are not observed in wild type *S. lycopersicum* (Bauer *et al.*, 2004a), although the occurrence of a range of wax esters accompanied by depletion of alkanes was reported in the *positional sterile* (*ps*) tomato mutant (Leide *et al.*, 2011). The wax esters observed here were particularly remarkable for the abundance of odd chain lengths. Analysis of arabidopsis mutants suggests that the wax ester biosynthesis pathway depends on two key enzymes. The first, CER4, is a fatty-acid CoA reductase that produces primary alcohols by reduction of CoA esters of VLCFAs. The second is WSD1, a protein of the WS/DGAT family that catalyzes the synthesis of wax esters from fatty acid CoA esters and primary alcohols. Since fatty acid elongation occurs by addition of two-carbon units and synthesis of alkanes occurs by loss of one carbon, the typical chain length distribution of acids and primary alcohols is even, while alkanes are predominantly odd in chain length (Figure 7; Samuels *et al.*, 2009). Following this pattern, as they are typically synthesized from fatty acids and primary alcohols, esters are typically also even in chain length. The abundance of odd-numbered esters observed here, despite the typical predominance of odd alkanes (Figure 5b,c), suggests an alternative biosynthetic route leading to odd-numbered esters. Analysis of the methanolyzed esters showed that the component responsible for the predominance of odd chain lengths was the alcohol moiety (Figure S2). Based on the existing model of wax ester biosynthesis, a relatively simple pathway that can be envisioned to explain the chain length distribution that we observed is depicted in Figure 7. First, synthesis of the even-chain length esters occurs through VLCFA reduction, catalyzed by an ortholog of CER4, followed by acyl transfer catalyzed by an ortholog of WSD1. This series of reactions is analogous to the known pathway in arabidopsis (Kunst and Samuels, 2009). The accumulation of esters in the *ps* mutant of *S. lycopersicum* (Leide *et al.*, 2011), and the occurrence of small amounts of primary alcohols in most of the species we examined (Figure 5a), suggests that these activities are present and that enhanced accumulation of their products may simply be a matter of variable expression of these enzymes.

The pathway leading to the odd chain length esters would be the same as that outlined above, except that the odd-chain primary alcohols would be synthesized by an alkane ω-hydroxylase. While hydroxylation of alkanes to yield secondary alcohols with an odd number of carbons is known to be catalyzed by CYP96A15 in arabidopsis (Greer *et al.*, 2007), an enzyme catalyzing ω-hydroxylation of alkanes is not yet known. The *Solanum* species provide a potentially excellent system to identify such an activity.

Genetic mapping of cuticle traits and future prospects

As a demonstration of the feasibility of mapping the genes underlying cuticular diversity in *Solanum* Sect. *Lycopersicon*, we selected a qualitative trait that clearly distinguishes *S. habrochaites* cuticles from those of *S. lycopersicum*. Although generally having a lower abundance of triterpenoids, *S. habrochaites* completely lacked all triterpenoids other than β-amyrin (Figure 5a,d). In the ILs that we analyzed, only LA3917 has the phenotype of the wild parent (Figure 6a). Since the introgressed genomic segments of this IL include the region on chromosome 12 encoding *SlTTS1* and *SlTTS2*, the two triterpene synthases responsible for wax triterpenoid biosynthesis in *S. lycopersicum*, these are promising candidates for genes underlying this aspect of cuticle diversity (Figure 6b). A simple loss of function in *TTS2*, leaving only *TTS1* functioning, would result in accumulation of solely β-amyrin (Figure 6c). Alternatively, since both *SlTTS1* and *SlTTS2* are very closely related, *SlTTS2* may be undergoing neofunctionalization in terms of product specificity following a tandem duplication, and *S. habrochaites TTS1* and *TTS2* may represent the ancestral state of a β-amyrin specific triterpene synthases. This second hypothesis is supported by the trend

towards increasing complexity and abundance of triterpenoid isomers with species that are more closely related to *S. lycopersicum* (Figure 5d). Resolution of this question would require biochemical characterization of *S. habrochaites TTS1* and *TTS2* and will be the target of future studies.

As previously mentioned, aside from evolutionary adaptation, environmental growth conditions can have a substantial effect on cuticle properties. Although all plants grown for the majority of the experiments in this study were grown simultaneously in the same conditions, we noticed a substantial difference in both the amount of cutin and the thickness of the cuticle of *S. lycopersicum* cv. M82, compared with our previous studies (Isaacson *et al.*, 2009), despite consistency in wax amount (Figure 2h, 4 and 5a). Similarly, although cuticular thickness is difficult to determine using SEM, the cuticles of plants grown in greenhouses in Israel for these experiments appear to be more substantial (Figure S1). We note that in both of these cases, these plants were grown in greenhouses with less sophisticated temperature control and may have been more stressed than the plants grown for light microscopy and chemical analysis in the present study. It is also worth noting that the substantial change in cuticle thickness and amount is similar to that observed with water-stressed arabidopsis plants (Kosma *et al.*, 2009). In *S. lycopersicum*, water stress has been shown to induce leaf wax biosynthesis and decrease cuticular transpiration, although cutin and fruit were not analyzed (Xu *et al.*, 1995). Taken together, it seems likely that there is an environmental component to induction of cuticle of biosynthesis in *Solanum* spp. that remains to be investigated. These results also suggest that future cuticle studies of wild species-derived QTL must be carefully designed to control for environmental influence.

An additional consideration is the diversity that may exist between accessions of the same species. There are more than 1,200 catalogued accessions of *Solanum* Sect. *Lycopersicon* (Moyle, 2008, http://trgr.ucdavis.edu) and their distribution into various subspecies and species is still being defined (Peralta *et al.*, 2008). In this study we focused on a single accession of each species, but there is likely value in investigating variation at the accession level, just as considerable cuticular diversity has been noted between cultivars of *S. lycopersicum* (Bauer *et al.*, 2004b).

Here we have shown that there is substantial diversity in the structure and chemical composition of the fruit cuticles of wild tomato species. Furthermore, despite the diversity, we have shown that the traits identified may be relatively simple in their genetic bases. *Solanum* Sect. *Lycopersicon* thus hits the ‘sweet spot’ of balancing recent evolutionary divergence with diversity that is required for future EEFG studies related to the fruit cuticle. We have shown that a desiccating environment is not likely to be a selective pressure for the evolution of a thicker fruit cuticle, since there was no association between species being endemic to arid environments and cuticle thickness. While the evolutionary mechanisms of other aspects of cuticle chemistry and morphology are still unclear, future genetic experiments aimed at correlating cuticle or fruit traits, such as water loss and pathogen resistance, with structural and chemical characteristics, will provide a means of discerning the complex interactions between cuticle structure and function.

Experimental procedures

Plant material

Seeds for all wild species were obtained from the Tomato Genetics Resource Center (UC Davis, http://tgrc.ucdavis.edu). For *S. lycopersicum*, the M82 cultivar was used (LA3475). The wild species accessions used were: *S. pimpinellifolium*, LA1589; *S. cheesmaniae*, LA0166; *S. chmielewskii*, LA1028; *S. neorickii*, LA2133; *S. habrochaites*, LA0407 and *S. pennellii*, LA0716. All species used for light microscopy, confocal microscopy and chemical

analysis were grown in the same greenhouse in Ithaca, NY under standard conditions. For SEM experiments, plants were grown in the greenhouse in Bet Dagan, Israel. The ILs were grown in the summer of 2009 in the field in Freeville, NY. Since the wild parent of the *S. habrochaites* ILs is the accession LA1777 (Monforte and Tanksley, 2000), this accession was also grown in the greenhouse for chemical analysis, which revealed that that there were no variations in cuticular triterpenoids between accessions (data not shown).

Microscopy

For light microscopy, tomato fruit pericarp tissue was fixed, embedded, cryosectioned, and post-fixed as described in (Buda *et al.*, 2009). Cryosections (4 μm) were melted on to VistaVision Histobond slides (VWR, www.vwr.com), dried and stained with Oil Red O (saturated in 60% isopropanol). Stain preparation and schedule was as described in Fukumoto and Fujimoto (2002): sections were rinsed with 50% isopropanol, followed by water, and mounted in water. Images were obtained using differential interference contrast (DIC) optics on an AxioImager A1 microscope equipped with an EC-Plan NeoFluar 40x/0.75 objective and an AxioCam Mrc color video camera (Zeiss, www.zeiss.com). For cuticle thickness measurements, sections were stained with Sudan IV (Buda *et al.*, 2009) and thickness was determined for each biological replicate, taking the average of 12 measurements (Figure 2). The average and standard error of the five biological replicates (fruits) is reported. For confocal microscopy and tomography, cryosections (30 μm) of fruit pericarp tissues were obtained and post-fixed as above, stained for 1 hour in Auramine O (0.1% w/v in 0.05 M Tris/HCl, pH 6.8) and mounted in water. Confocal microscopy and z-stack collection was performed as outlined in (Buda *et al.*, 2009). Z-stacks were pre-processed using LAS-AF v 1.8.2 (Leica, www.leicamicrosystems.com) and Image J (http://rsbweb.nih.gov) software. Cuticle image stacks were then assembled into 3D volume renderings using OsiriX software (Rosset *et al.*, 2004). SEM microscopy was performed as described in Hovav *et al.*, (2007).

Cuticle isolation

Mature fruits were harvested and three orthogonal diameters of each fruit were determined using calipers. The average of the three diameters was used to calculate the surface area, assuming a perfect sphere of this average diameter. For each biological replicate, 5–10 fruits were combined and manually dissected to remove the seeds and most of the pericarp. Cuticles were then isolated by the enzymatic method as previously described (Isaacson *et al.*, 2009).

Wax chemical analysis

Dried cuticles were spiked with tetracosane as an internal standard and extracted three times with a small volume of chloroform. The extracts were pooled and an aliquot was dried by heating under a gentle stream of nitrogen. The wax mixture was derivatized and subjected to GC analysis as previously described (Wang *et al.*, 2011) with the following exceptions: GC-FID quantitative analysis was performed on a model 6850 gas chromatograph (Agilent, www.agilent.com), while GC-MS qualitative analysis was as previously described. Since wax extracts from enzymatically isolated cuticles typically contain C16 and C18 fatty acids and other lipophilic contaminants absorbed from cellular debris during cuticle isolation (Schönherr and Riederer, 1986), quantification only considered peaks eluting after the C27 *n*-alkane (~14 min).

To address the composition of wax esters observed in some species, the *S. neorickii* wax extract was fractionated by K6 silica gel TLC (Whatman, www.whatman.com) developed with chloroform. The ester band was recovered and eluted with chloroform. Methanolysis with sodium methoxide and subsequent derivatization with BSTFA/pyridine yielded a

mixture of fatty alcohol TMS ethers and fatty acid methyl esters, which were identified by GC-MS and quantified by GC-FID as previously described.

Cutin chemical analysis

A protocol based on Bonaventure *et al.* (2004) was used for cutin analysis with some modifications. The dewaxed cuticular membranes were dried overnight and placed in a glass vial along with ω-pentadecalactone and methyl heptadecanoate as internal standards. A 10 mL reaction mixture, consisting of 6 mL methanol, 1.5 mL methyl acetate and 2.5 mL of 30% sodium methoxide in methanol, was added to each sample. The vials were capped and heated to 60˚C for 2 hours. After cooling to room temperature, 20 mL of diethyl ether and 2.5 mL of glacial acetic acid were added. To this, 5 mL of aqueous buffer (0.9% NaCl, 100 mM Tris pH 8.0) was added and the tubes were mixed thoroughly by vortexing. The phases were separated by centrifugation (2 min at 1500 x g) and an aliquot of the upper organic phase was removed. This was combined with an equal volume of 0.9% NaCl, vortexed and centrifuged again. An aliquot of the organic upper phase was taken and transferred to a conical reaction vial. An equal volume of 2,2-dimethoxypropane was added to dry the sample and the vial was capped and incubated at 50˚C for 15 minutes. The solvent was evaporated by heating under a gentle stream of nitrogen before derivatization of the sample with 10 μL BSTFA and 10 μL pyridine. The reaction was heated for 10 minutes at 90˚C and dried again under nitrogen. The sample, resuspended in chloroform, was then subjected to GC-FID analysis as described for wax analysis. Compounds were identified by running the same samples on GC-MS and comparison to reference spectra from Holloway (1982).

Supplementary Material

Refer to Web version on PubMed Central for supplementary material.

Acknowledgments

We thank Jonathan Fuller and Samuel Mullin for technical assistance and Dr. J. Giovannoni for providing fruit from the *S. habrochaites* ILs. We thank Dr. S. Knapp for helpful comments and discussion. Confocal imaging was performed at the Plant Cell Imaging Center at the Boyce Thompson Institute which is supported by grants from the National Science Foundation (DBI-0618969) and the TRIAD foundation. This work was supported by grants from the National Science Foundation (Plant Genome Program; DBI-0606595), the United States-Israel Binational Agricultural Research and Development Fund (IS-4234-09), U.S.-Israel Binational Science Foundation (2005-168), a CUAES-Hatch grant (NYC-184462), the Canada Research Chairs Program and a Special Research Opportunities Grant from the Natural Sciences and Engineering Council of Canada (327937-2005). T.H.Y. was partly supported by a National Institutes of Health chemistry/biology interface training grant (T32 GM008500).

Abbreviations

AL	Anticlinal lamellae
AP	Anticlinal peg
CR	Cellular remnants
DIC	Differential interference contrast
EEFG	Ecological and evolutionary functional genomics
GC-FID	Gas chromatography-flame ionization detector
GC-MS	Gas chromatography-mass spectrometry
IL	Introgression line
IST	Internal surface topology

N	Nucleus
nd	Not detected
ps	Positional sterile
QTL	Quantitative trait loci
SD	Subepidermal cuticular deposit
T	Thickness
TLC	Thin layer chromatography

References

Baker, EA.; Bukovac, MJ.; Hunt, GM. Composition of tomato fruit cuticle as related to fruit growth and development. In: Cutler, DF.; Alvin, KL.; Price, CE., editors. The Plant Cuticle. London: Academic Press; 1982. p. 33-44.

Barthlott W, Neinhuis C. Purity of the sacred lotus, or escape from contamination in biological surfaces. Planta. 1997; 202:1–8.

Bauer S, Schulte E, Thier H. Composition of the surface wax from tomatoes: I. Identification of the components by GC/MS. Eur. Food Res. Technol. 2004a; 219:223–228.

Bauer S, Schulte E, Thier H. Composition of the surface wax from tomatoes: II. Quantification of the components at the ripe red stage and during ripening. Eur. Food Res. Technol. 2004b; 219:487–491.

Bonaventure G, Beisson F, Ohlrogge J, Pollard M. Analysis of the aliphatic monomer composition of polyesters associated with Arabidopsis epidermis: occurrence of octadeca-*cis*-6, *cis*-9-diene-1,18-dioate as the major component. Plant J. 2004; 40:920–930. [PubMed: 15584957]

Buda GJ, Isaacson T, Matas AJ, Paolillo DJ, Rose JK. Three-dimensional imaging of plant cuticle architecture using confocal scanning laser microscopy. Plant J. 2009; 60:378–385. [PubMed: 19563439]

Buschhaus C, Jetter R. Composition differences between epicuticular and intracuticular wax substructures: how do plants seal their epidermal surfaces? J. Exp. Bot. 2011; 62:841–853. [PubMed: 21193581]

Croteau R, Kolattukudy PE. Biosynthesis of hydroxyfatty acid polymers. Enzymatic epoxidation of 18-hydroxyoleic acid to 18-hydroxy-*cis*-9,10-epoxystearic acid by a particulate preparation from spinach (*Spinacia oleracea*). Arch. Biochem. Biophys. 1975a; 170:61–72. [PubMed: 240325]

Croteau R, Kolattukudy PE. Biosynthesis of hydroxyfatty acid polymers. Enzymatic hydration of 18-hydroxy-*cis*-9,10-epoxystearic acid to *threo*-9,10,18-trihydroxystearic acid by a particulate preparation from apple (*Malus pumila*). Arch. Biochem. Biophys. 1975b; 170:73–81. [PubMed: 240326]

Dillon MO. Origins and diversity of the lomas formations in the Atacama and Peruvian Deserts of western South America. Am. J. Bot. 1989; 76:212. Abstract.

Edwards D. Cells and tissues in the vegetative sporophytes of early land plants. New Phytol. 1993; 125:225–247.

Eshed Y, Zamir D. An introgression line population of Lycopersicon pennellii in the cultivated tomato enables the identification and fine mapping of yield-associated QTL. Genetics. 1995; 141:1147–1162. [PubMed: 8582620]

Fernandez V, Khayet M, Montero-Prado P, et al. New insights into the properties of pubescent surfaces: peach fruit as a model. Plant Physiol. 2011; 156:2098–2108. [PubMed: 21685175]

Franke R, Briesen I, Wojciechowski T, Faust A, Yephremov A, Nawrath C, Schreiber L. Apoplastic polyesters in *Arabidopsis* surface tissues–a typical suberin and a particular cutin. Phytochem. 2005; 66:2643–2658.

Fukumoto S, Fujimoto T. Deformation of lipid droplets in fixed samples. Histochem. Cell Biol. 2002; 118:423–428. [PubMed: 12432454]

Graca J, Schreiber L, Rodrigues J, Pereira H. Glycerol and glyceryl esters of omega-hydroxyacids in cutins. Phytochem. 2002; 61:205–215.

Greer S, Wen M, Bird D, Wu X, Samuels L, Kunst L, Jetter R. The cytochrome P450 enzyme CYP96A15 is the midchain alkane hydroxylase responsible for formation of secondary alcohols and ketones in stem cuticular wax of Arabidopsis. Plant Physiol. 2007; 145:653–667. [PubMed: 17905869]

Holloway, PJ. The chemical constiution of plant cutins. In: Cutler, DF.; Alvin, KL.; Price, CE., editors. The Plant Cuticle. London: Academic Press; 1982. p. 45-85.

Hovav R, Chehanovsky N, Moy M, Jetter R, Schaffer AA. The identification of a gene (*Cwp1*), silenced during *Solanum* evolution, which causes cuticle microfissuring and dehydration when expressed in tomato fruit. Plant J. 2007; 52:627–639. [PubMed: 17877702]

Isaacson T, Kosma DK, Matas AJ, et al. Cutin deficiency in the tomato fruit cuticle consistently affects resistance to microbial infection and biomechanical properties, but not transpirational water loss. Plant J. 2009; 60:363–377. [PubMed: 19594708]

Javelle M, Vernoud V, Rogowsky PM, Ingram GC. Epidermis: the formation and functions of a fundamental plant tissue. New Phytol. 2011; 189:17–39. [PubMed: 21054411]

Jeffree, CE. The fine structure of the plant cuticle. In: Riederer, M.; Müller, C., editors. Biology of the Plant Cuticle. Oxford, UK: Blackwell; 2006. p. 11-125.

Jenks MA, Ashworth EN. Plant epicuticular waxes: function, production and genetics. Hortic. Rev. 1999; 23:1–68.

Jetter, R.; Kunst, L.; Samuels, AL. Composition of plant cuticular waxes. In: Riederer, M.; Müller, C., editors. Biology of the Plant Cuticle. Oxford, UK: Blackwell; 2006. p. 145-181.

Kolattukudy PE. Polyesters in higher plants. Adv. Biochem. Eng. Biotechnol. 2001; 71:1–49. [PubMed: 11217409]

Kolattukudy PE, Walton TJ, Kushwaha RP. Biosynthesis of the C18 family of cutin acids: omega-hydroxyoleic acid, omega-hydroxy-9,10-epoxystearic acid, 9,10,18-trihydroxystearic acid, and their delta12-unsaturated analogs. Biochemistry. 1973; 12:4488–4498. [PubMed: 4356240]

Kosma DK, Bourdenx B, Bernard A, Parsons EP, Lu S, Joubes J, Jenks MA. The impact of water deficiency on leaf cuticle lipids of Arabidopsis. Plant Physiol. 2009; 151:1918–1929. [PubMed: 19819982]

Kunst L, Samuels L. Plant cuticles shine: advances in wax biosynthesis and export. Curr. Opin. Plant Biol. 2009; 12:721–727. [PubMed: 19864175]

Leide J, Hildebrandt U, Reussing K, Riederer M, Vogg G. The developmental pattern of tomato fruit wax accumulation and its impact on cuticular transpiration barrier properties: Effects of a deficiency in a beta-ketoacyl-coenzyme A synthase (LeCER6). Plant Physiol. 2007; 144:1667–1679. [PubMed: 17468214]

Leide J, Hildebrandt U, Vogg G, Riederer M. The *positional sterile* (*ps*) mutation affects cuticular transpiration and wax biosynthesis of tomato fruits. J Plant Physiol. 2011; 168:871–877. [PubMed: 21242016]

Li-Beisson Y, Pollard M, Sauveplane V, Pinot F, Ohlrogge J, Beisson F. Nanoridges that characterize the surface morphology of flowers require the synthesis of cutin polyester. Proc. Natl. Acad. Sci. U.S.A. 2009; 106:22008–22013. [PubMed: 19959665]

Mitchell-Olds T, Feder M, Wray G. Evolutionary and ecological functional genomics. Heredity. 2008; 100:101–102. [PubMed: 18212796]

Monforte AJ, Tanksley SD. Development of a set of near isogenic and backcross recombinant inbred lines containing most of the *Lycopersicon hirsutum* genome in a *L. esculentum* genetic background: a tool for gene mapping and gene discovery. Genome. 2000; 43:803–813. [PubMed: 11081970]

Moyle LC. Ecological and evolutionary genomics in the wild tomatoes (*Solanum* sect. *Lycopersicon*). Evolution. 2008; 62:2995–3013. [PubMed: 18752600]

Mueller LA, Solow TH, Taylor N, et al. The SOL Genomics Network: a comparative resource for Solanaceae biology and beyond. Plant Physiol. 2005; 138:1310–1317. [PubMed: 16010005]

Nakazato T, Warren DL, Moyle LC. Ecological and geographic modes of species divergence in wild tomatoes. Am. J. Bot. 2010; 97:680–693. [PubMed: 21622430]

Niklas, KJ. Paleobiochemical techniques and their applications to paleobotany. In: Reinhold, L.; Harborne, JB.; Swain, T., editors. Progress in Phytochemistry. Vol. Vol. 6. Oxford, UK: Pergamon Press; 1980. p. 143-181.

Peralta IE, Spooner DM, Knapp S. Taxonomy of wild tomatoes and their relatives (*Solanum* sect. *Lycopersicoides*, sect. *Juglandifolia*, sect. *Lycopersicon*; Solanaceae). Syst. Bot. Monog. 2008; 84:1–186.

Pfündel, EE.; Agati, G.; Cerovic, ZG. Optical properties of plant surfaces. In: Riederer, M.; Müller, C., editors. Biology of the Plant Cuticle. Oxford, UK: Blackwell; 2006. p. 216-249.

Pinot F, Beisson F. Cytochrome P450 metabolizing fatty acids in plants: characterization and physiological roles. FEBS J. 2011; 278:195–205. [PubMed: 21156024]

Pollard M, Beisson F, Li Y, Ohlrogge JB. Building lipid barriers: biosynthesis of cutin and suberin. Trends Plant Sci. 2008; 13:236–246. [PubMed: 18440267]

Prudent M, Causse M, Genard M, Tripodi P, Grandillo S, Bertin N. Genetic and physiological analysis of tomato fruit weight and composition: influence of carbon availability on QTL detection. J. Exp. Bot. 2009; 60:923–937. [PubMed: 19179559]

Reina-Pinto JJ, Yephremov A. Surface lipids and plant defenses. Plant Physiol. Biochem. 2009; 47:540–549. [PubMed: 19230697]

Riederer M, Schreiber L. Protecting against water loss: analysis of the barrier properties of plant cuticles. J. Exp. Bot. 2001; 52:2023–2032. [PubMed: 11559738]

Rosset A, Spadola L, Ratib O. OsiriX: an open-source software for navigating in multidimensional DICOM images. J. Digit. Imaging. 2004; 17:205–216. [PubMed: 15534753]

Samuels AL, Kunst L, Jetter R. Sealing plant surfaces: cuticular wax formation by epidermal cells. Annu. Rev. Plant Biol. 2008; 59:683–707. [PubMed: 18251711]

Sauveplane V, Kandel S, Kastner PE, Ehlting J, Compagnon V, Werck-Reichhart D, Pinot F. Arabidopsis thaliana CYP77A4 is the first cytochrome P450 able to catalyze the epoxidation of free fatty acids in plants. FEBS J. 2009; 276:719–735. [PubMed: 19120447]

Schauer N, Zamir D, Fernie AR. Metabolic profiling of leaves and fruit of wild species tomato: a survey of the *Solanum lycopersicum* complex. J. Exp. Bot. 2005; 56:297–307. [PubMed: 15596477]

Schönherr J, Riederer M. Plant cuticles sorb lipophilic compounds during enzymatic isolation. Plant Cell Environ. 1986; 9:459–466.

Seo PJ, Lee SB, Suh MC, Park MJ, Go YS, Park CM. The MYB96 transcription factor regulates cuticular wax biosynthesis under drought conditions in Arabidopsis. Plant Cell. 2011; 23:1138–1152. [PubMed: 21398568]

Vogg G, Fischer S, Leide J, Emmanuel E, Jetter R, Levy AA, Riederer M. Tomato fruit cuticular waxes and their effects on transpiration barrier properties: functional characterization of a mutant deficient in a very-long-chain fatty acid β-ketoacyl-CoA synthase. J. Exp. Bot. 2004; 55:1401–1410. [PubMed: 15133057]

Walton, TJ. Waxes, cutin and suberin. In: Harwood, JL.; Bowyer, JR., editors. Methods in plant biochemistry: lipids, membranes and aspects of photobiology. London: Academic Press; 1990. p. 105-158.

Wang Z, Guhling O, Yao R, Li F, Yeats TH, Rose JK, Jetter R. Two oxidosqualene cyclases responsible for biosynthesis of tomato fruit cuticular triterpenoids. Plant Physiol. 2011; 155:540–552. [PubMed: 21059824]

Xu HL, Gauthier L, Gosselin A. Stomatal and cuticular transpiration of greenhouse tomato plants in response to high solution electrical-conductivity and low soil-water content. J. Am. Soc. Hortic. Sci. 1995; 120:417–422.

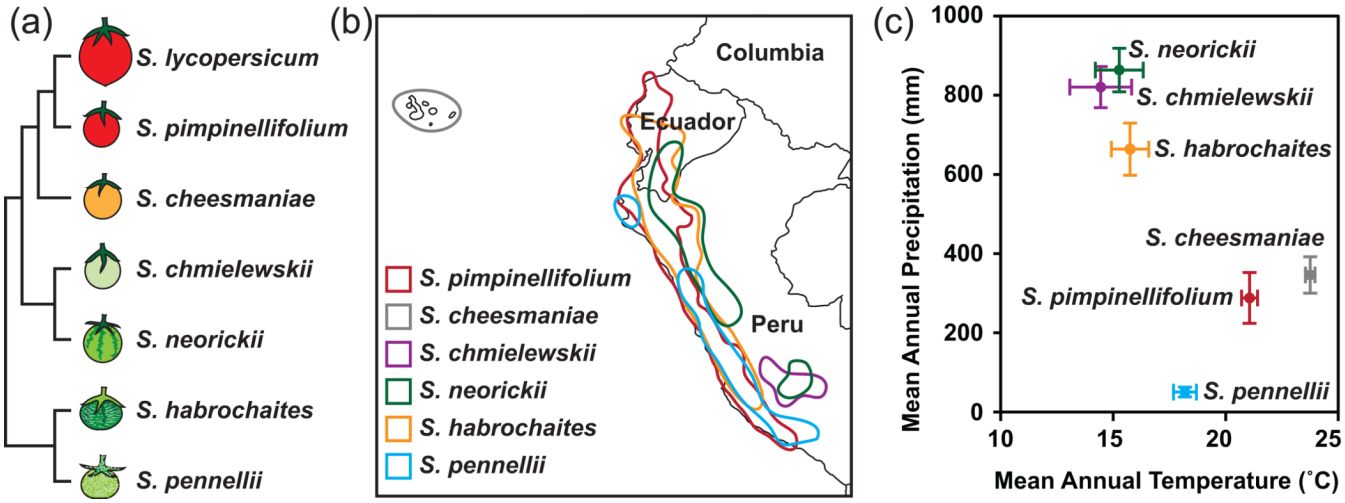

Figure 1. Phylogenetic and ecological context of the species in this study

(a) Phylogenetic tree of the seven *Solanum* species considered here, based on Rodriguez *et al.* 2009. (b) Geographical distribution of the six wild species based on the occurrence records of the Tomato Genetic Resource Center (TGRC, UC Davis, http://tgrc.ucdavis.edu). (c) Climate space plot of each species (mean and 95% CI) based on records for known geographical locations of each species (TGRC), using methods described in Nakazato *et al.* (2010).

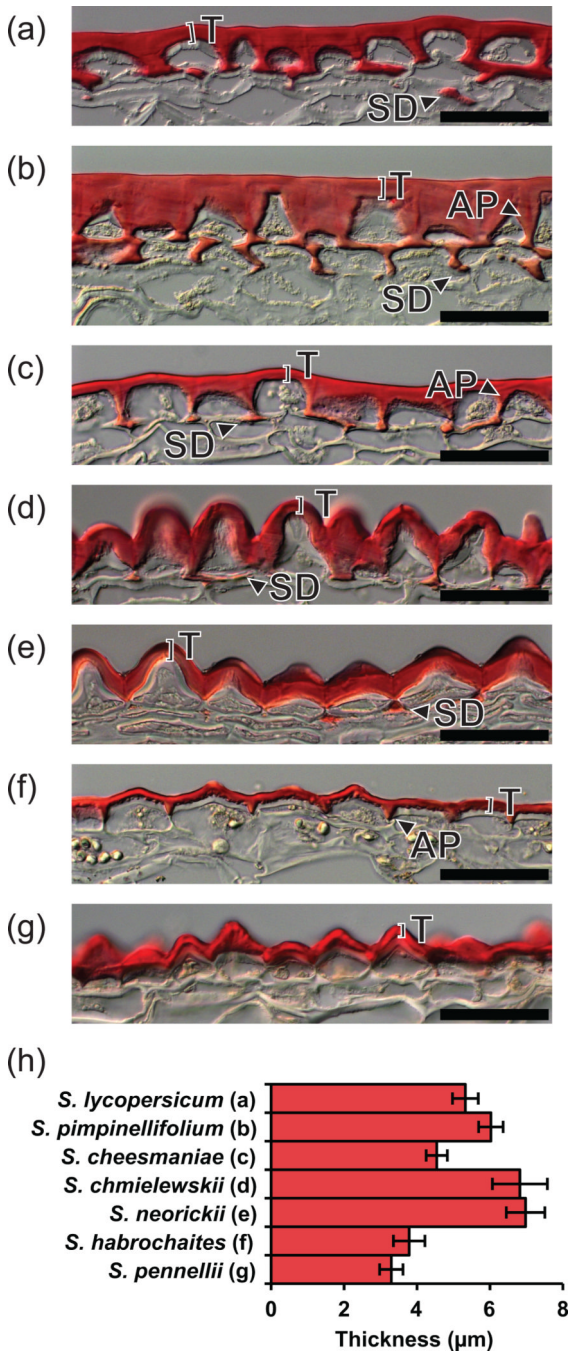

Figure 2. Two-dimensional cuticle morphology

(a–g) Light micrographs of sections of the fruit surface of tomato (*S. lycopersicum*) and six wild relatives, showing the cuticle stained with Oil red O. Scale bars = 50 µm. T, Thickness; SD, Subepidermal cuticular deposit; AP, Anticlinal peg. The species represented in each panel is shown in panel H of this figure. (h) Cuticle thickness measurements. Measurements were made above the center of each epidermal cell as indicated by bars labeled “T” in panels A–G. Error bars are S.E. for n=5.

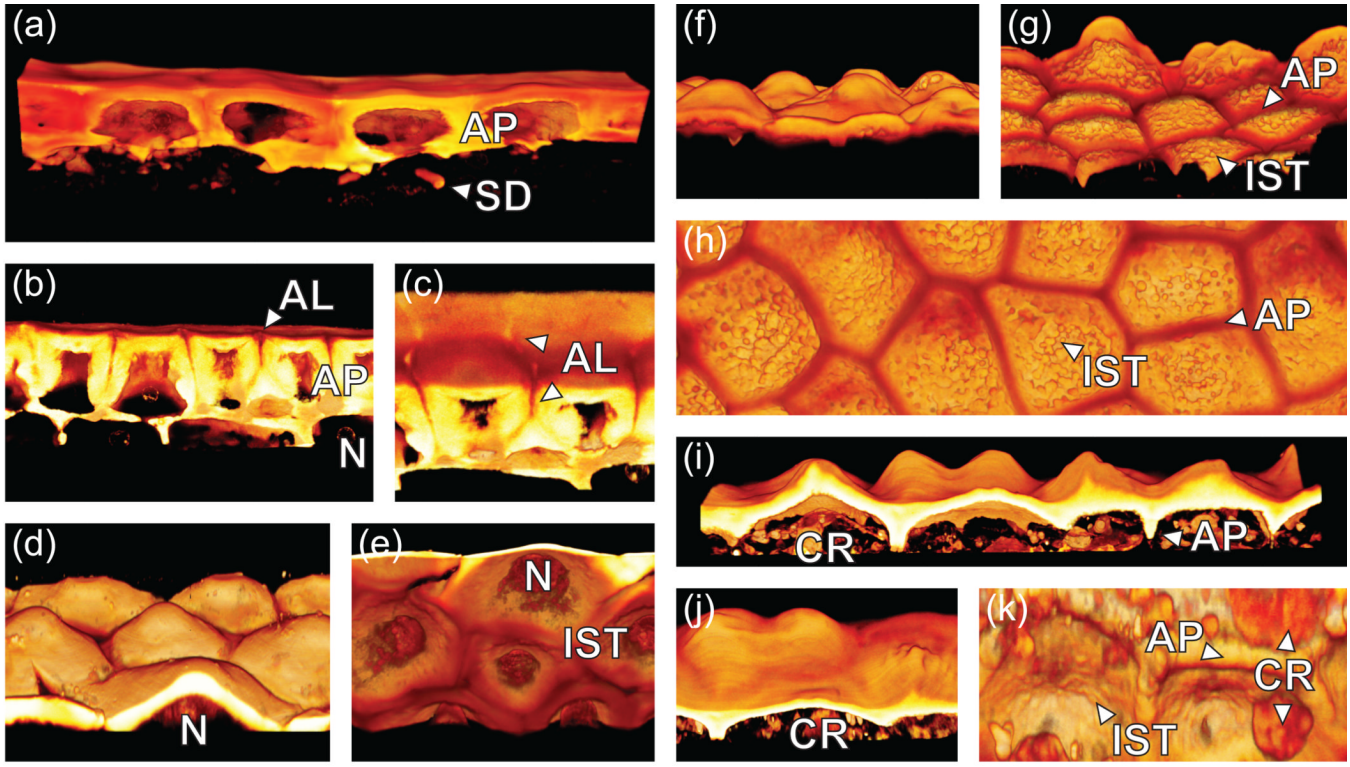

Figure 3. Three-dimensional cuticle morphology

Three-dimensional volume renderings constructed from confocal Z-stacks. (a) *S. lycopersicum*. (b–c) *S. pimpinellifolium*. (d–e) *S. neorickii*. (f–h) *S. habrochaites*. (i–k) *S. pennellii*. AP, Anticlinal peg; SD, Subepidermal cuticular deposit; AL, Anticlinal lamellae; N, Nucleus; IST, Internal surface topology; CR, Cellular remnants.

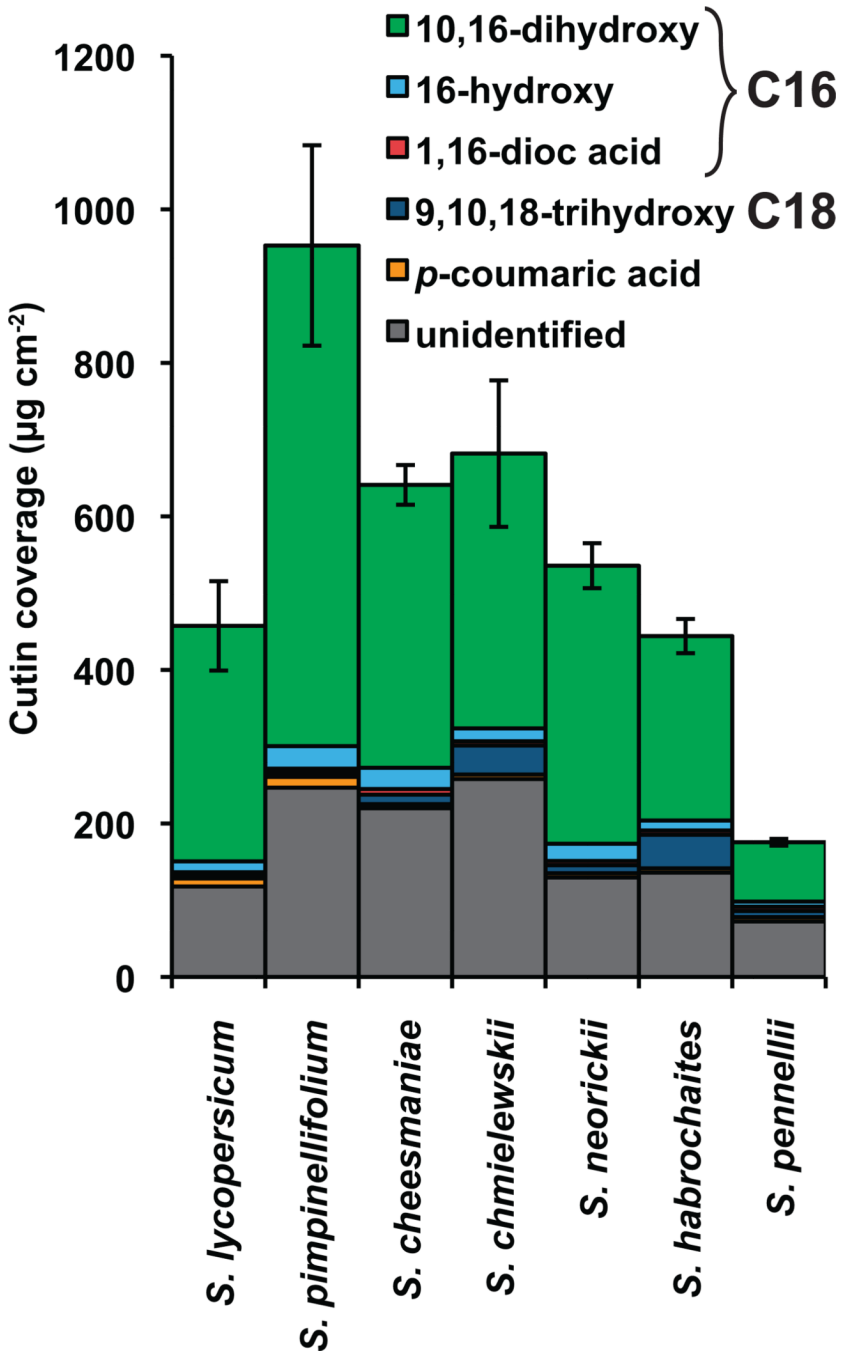

Figure 4. Cutin chemical composition

Monomer composition of cutin from fruit cuticles of various *Solanum* species. Error bars are S.E. for n=3.

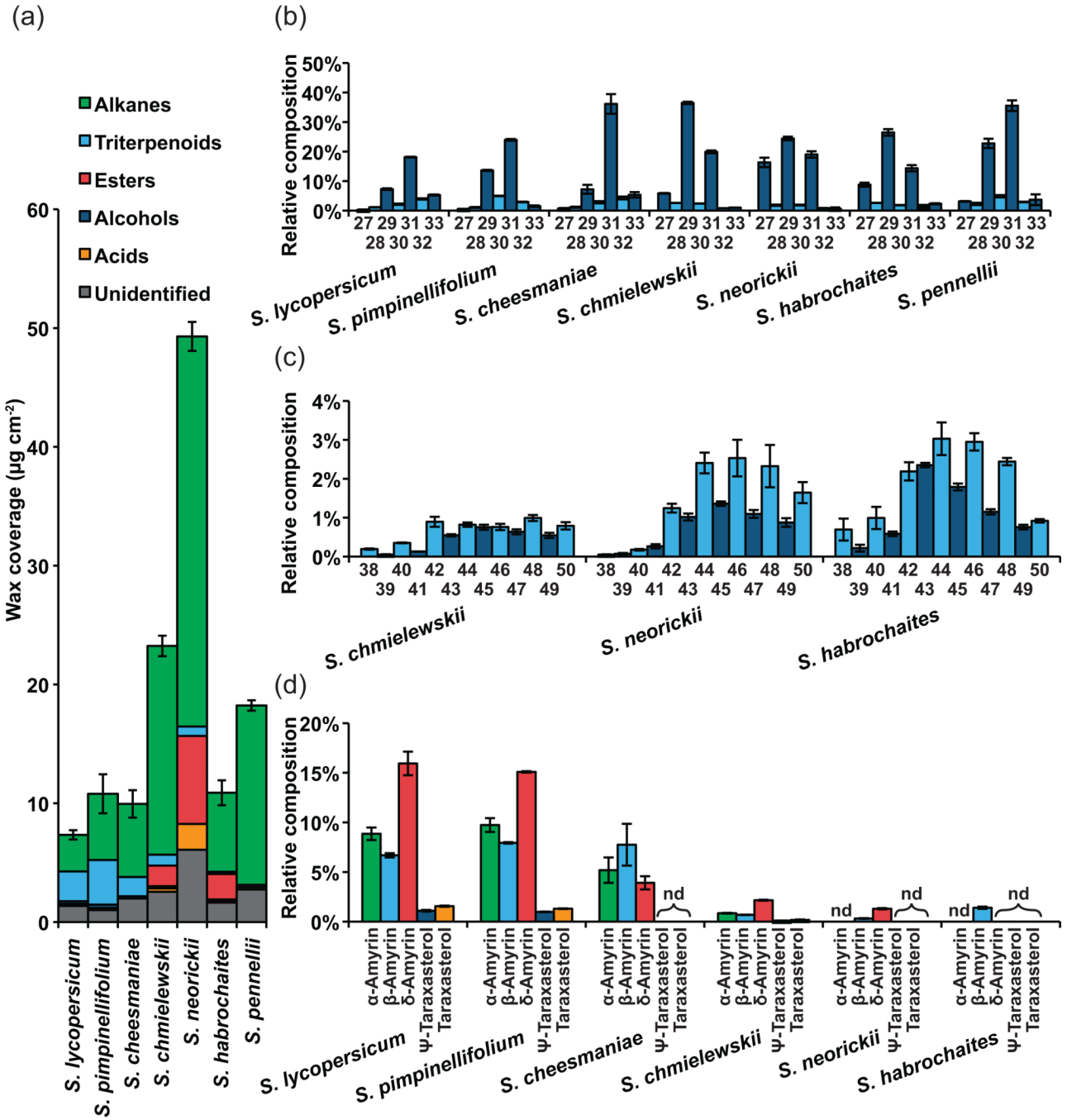

Figure 5. Wax chemical composition

(a) Total wax and compound class coverage for each species. (b) *n*-Alkane chain length distribution for each species. The number of carbons is indicated below. (c) Alkyl ester chain length distribution for the three species exhibiting this compound class. The number of carbons is indicated below. (d) Triterpenoid isomer distribution for the six species where triterpenoids were observed. nd, Not detected. Error bars are S.E. for n=3.

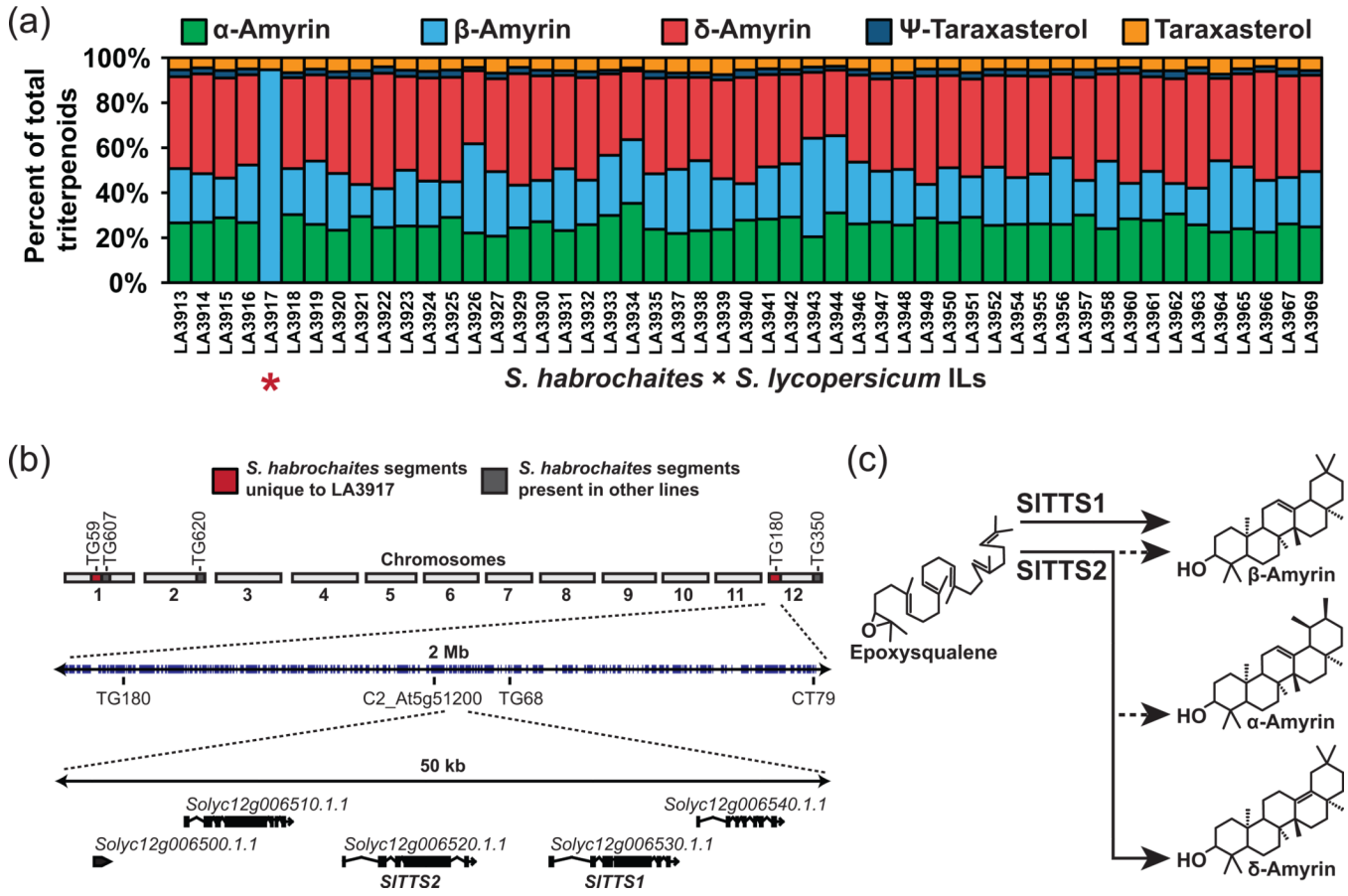

Figure 6. Genetic mapping of α- and δ-amyrin synthesis

(a) Relative contribution of triterpenoid isomers to the total cuticular triterpenoids for 51 *S. habrochaites* introgression lines in a *S. lycopersicum* background. LA3917 (indicated by *) had no detectable α- or δ-amyrin. (b) The genetic architecture of LA3917. The introgressed segments surrounding the markers TG59 and TG180 are uniquely represented in this line (shaded in red). The latter segment contains the tandem loci SlTTS1 and SlTTS2 that encode the two triterpene synthases of *S. lycopersicum*. (c) The isomer specificity of the two triterpene synthases of *S. lycopersicum*, SlTTS1 and SlTTS2. SlTTS1 synthesizes β-amyrin exclusively while SlTTS2 synthesizes primarily δ-amyrin and lesser amounts of α- and β-amyrin.

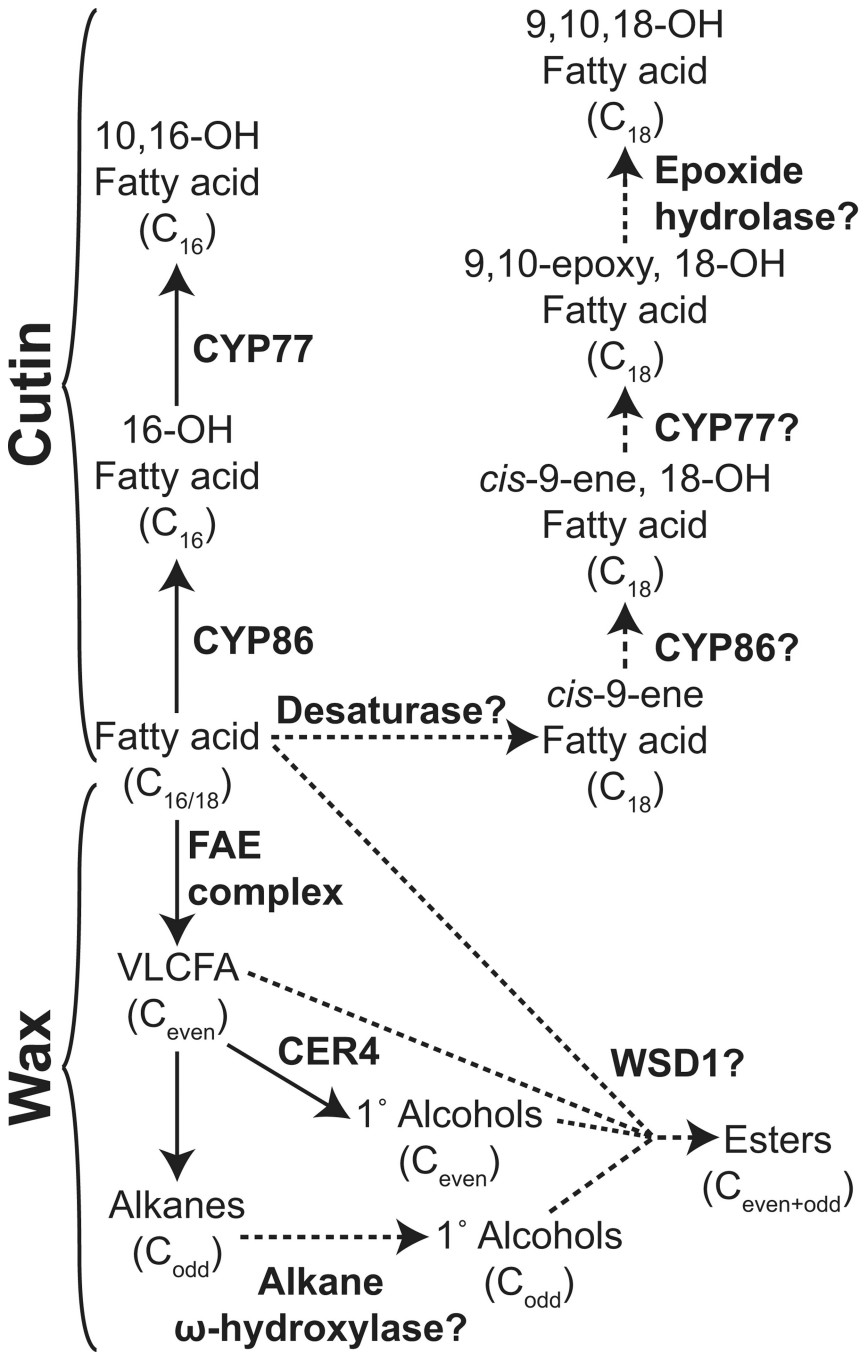

Figure 7. Biosynthesis of acyl lipids found in the cuticles of *Solanum spp*

Proposed synthesis pathways of lipid classes not found in *S. lycopersicum* are shown with dashed lines. For simplicity, coenzyme A is omitted from the diagram. FAE, fatty acid elongase; VLCFA, very long chain fatty acid.